Slender RC Columns Strengthened with a Novel Hybrid Strengthening System of External Longitudinal and Transverse FRPs

Koosha Khorramian[1] and Pedram Sadeghian[2]

ABSTRACT: In this study, the performance of slender circular concrete columns strengthened with a novel hybrid system of longitudinally bonded prefabricated fiber-reinforced polymer (FRP) laminates and transverse FRP wrapping is investigated. The novelty of the hybrid system is to improve the load carrying capacity of slender steel reinforced concrete (RC) columns under eccentric axial compression by providing high modulus longitudinal carbon FRP (CFRP) laminates through enhancing the flexural stiffness of the slender column, and laterally support the longitudinal laminates by FRP wraps to prevent debonding and local buckling. A total of 6 large scale circular slender RC columns with the diameter of 260 mm and the length of 3048 mm were tested under combined axial and flexural loads. The results showed that, for the strengthening of the slender columns, the hybrid system is a more effective strengthening system than wrapping controlling second-order deformations due the slenderness effect and enhancing the load bearing capacity. Also, the performance of the system was further investigated using an analytical-numerical model considering the second-order deformations of the slender columns. The model considered nonlinearity in material and confinement effects plus the geometrical nonlinearity via an iterative second-order analysis. The model was verified against experimental data from the current study (hybrid system) and an independent study (wrapping system) and showed a good agreement with the test results. Then, a comprehensive parametric study was conducted to study

[1] PhD Candidate, Department of Civil and Resource Engineering, Dalhousie University, D301, 1360 Barrington street, Halifax, NS, B3H 4R2 Canada (corresponding author). koosha.khorramian@dal.ca
[2] Associate Professor and Canada Research Chair in Sustainable Infrastructure, Department of Civil and Resource Engineering, Dalhousie University, B233B, 1360 Barrington Street, Halifax, NS, B3H 4R2 Canada, Pedram.Sadeghian@dal.ca

the effect of various parameters including slenderness ratio, load eccentricity, longitudinal and transverse FRP reinforcement ratios, concrete strength, and column diameter on the performance of slender RC columns strengthened with the hybrid system. It was found that the hybrid strengthening system was more effective for RC columns with high slenderness ratios, high load eccentricities, and low concrete strength.

DOI: 10.1061/(ASCE)ST.1943-541X.0003142

KEYWORDS: slender; concrete columns; strengthening; Fiber-reinforced polymer (FRP); hybrid; wrapping.

INTRODUCTION

Strengthening of the concrete columns with FRP wrapping is very frequent in the industry because of ease of installation and its performance in the enhancement of existing concrete columns. Although the wrapping system is effective for concentrically loaded columns (Nanni and Bradford, 1995; Pessiki et al., 2001; Xiao and Wu, 2000; Cui and Sheikh, 2010; Smith et al., 2010), it is not as effective for eccentrically loaded columns and researchers reported a reduction in the effectiveness of FRP wrapping for circular concrete columns loaded under eccentric loading (Parvin and Wang, 2001; Hadi, 2006; Bisby and Ranger, 2010; El Maaddawy et al., 2010; Al-Nimry and Soman, 2018). Also, ACI-440.2R-17 (2017) limits the effective rupture strain of FRP wraps to 0.004 mm/mm where the load eccentricities are more than 10% of the diameter of the column to account for the effect of the load eccentricity. To study the effectiveness of wrapping on combined flexural and axial loadings, many experimental studies have been conducted on eccentrically loaded wrapped concrete columns (Li et al., 2003; Tao et al., 2004; El-Maaddawy, 2009; Wu and Jiang, 2013; Wu and Cao, 2017; Carrazedo and de Hanai, 2017; Wang et al., 2018, Lin et al., 2020) and slender columns (Pan et al., 2007; Karimi et al., 2012; Chikh et al., 2012).

From experimental tests of eccentrically loaded wrapped concrete columns, it was observed that for compression side, the hoops strain is highest, and by moving from compression side to tension side, the hoop strain decreases and its corresponding confinement effect (Bisby and Ranger, 2010; Fitzwilliam and Bisby, 2010). The lack of effectiveness of the wrapping system for eccentric loading can be explained by the equilibrium in the section for eccentric loading. While for the concentric loading, the internal forces are all in compression, for eccentric loading moment equilibrium of the section requires both tension and compression elements. Since the wrapping is effective in enhancing the resultant of the internal compressive forces, and it does not change the tension side, even its compression effect cannot change the capacity of the column. Because the concrete is weak in tension, the presence or absence of confinement in compression is not effective for the eccentric loading due to lack of strengthening element s in the tension side of the column. Therefore, it can be concluded that the compression side would be over-reinforced by using the wrapping system alone. Thus, adding additional longitudinal FRP strips to the tension side of the columns can make the wrapping more effective in compression by providing the required elements for the equilibrium of the system. On the other hand, many researchers have been evaluated the strengthening performance of CFRP laminates on the tensile side of concrete beams (Shahawy et al., 1996; Triantafillou and Plevris, 1992; Sharif et al., 1994; Ashour et al., 2004), in which the tensile strips helped the increase of the flexural capacity of the system. However, due to the nature of the loading for the columns, the direction of the eccentricity may change and is not be certain. Thus, the compression side or tension side may vary during the life of the structure. Thus, considering a symmetric distribution of the longitudinal FRP strips can be considered to compromise the nature of the eccentricity direction. Therefore, some of the strips would be in compression. The advantage of using strips in compression is to increase the resultant of the

internal compressive forces which eliminates the need for wrapping the column. However, using longitudinal fibers in compression leads to micro buckling of fibers if any void is available in the resin (ACI 440.2R-17, 2017), and the contribution of FRPs in compression have been neglected by the design guidelines (CSA S806; 2012, ACI 440.2R, 2017; ACI 440.1R, 2015) due to lack of tests data. This study shows that longitudinal FRP strips are able to take significant compression contributing to the flexural stiffness of slender columns before crushing.

On the other hand, many researchers studied the effect of longitudinal FRP elements using different strengthening techniques. The techniques included wet layout system for longitudinal external FRP sheets (Tan, 2002; Hadi, 2007; Issa et al., 2009; Fitzwilliam and Bisby, 2010; Siddiqui et al., 2014; Siddiqui et al., 2020), near-surface mounted (NSM) technique (Gadjosova and Bilcik, 2013; Khorramian and Sadeghian, 2019), a combination of NSM and transverse wrapping (El-Maaddawy and El-Dieb, 2011; Quiertant, and Clement; 2011; Bournas and Triantafillou, 2013), longitudinal FRP sheets on grooves (Torabian and Mostofinejad, 2017; NoroozOlyaee and Mostofinejad, 2019; Saljoughian and Mostofinejad, 2020), and a hybrid system of bonded premanufactured FRPs with transverse wrapping (Khorramian and Sadeghian, 2018a, 2018b, and 2018c; Khorramian 2020). The results of studies for the effect of the longitudinal elements showed an increase in the capacity of the columns using longitudinal elements if sufficient transverse support is provided. However, when fabrics used as longitudinal reinforcement, longitudinal fibers in compression are prone to micro buckling (ACI 440.2R-17, 2017), and when the NSM system is used the percentage of the premanufactured laminated strips are limited due to the spacing limitations between the grooves. To have a more effective system, higher reinforcement ratios of longitudinal premanufactured strips can be provided by bonding them directly to the surface and support them transversely by wrapping. Higher reinforcement

ratios of longitudinal elements are required to add flexural rigidity and reduce the secondary moment effects. Also, providing higher reinforcement ratios, especially in the tension side, increase the effectiveness of the confining device in compression by providing the requirement for section equilibrium, as explained earlier. Thus, for the hybrid system, there are two major contributors in compression including confined concrete and the longitudinal strips in compression, and one major contributor in tension (i.e., longitudinal strips in tension). To study the hybrid system for the strengthening of eccentrically loaded slender columns, two different reinforcement ratios for longitudinal strips and two different wrapping stiffness were studied experimentally. Also, an analytical-numerical model was developed, and a parametric study was conducted on the effective parameters which control the behavior of the hybrid system. It should be noted that the scope of the current study is limited to the pin-ended concrete columns for which the maximum bending moment is at the middle of the columns, and, also, for the columns in a sway frame which were not expected to have maximum moments at the ends of the column. For columns in non-sway frames, or columns with different boundary condition which required maximum moment at the ends of the columns, the anchorage of the longitudinal FRPs should be studied which is out of the scope of the current study and requires a separate study.

RESEARCH SIGNIFICANCE

The novelty of the current study is testing and characterizing the behavior of a hybrid strengthening system of external longitudinal and transverse FRPs to alter the failure mode of slender RC columns from global buckling, or excessive second-order lateral deformations, to material failure with significantly less deformations and second-order moments. The gain is achieved by increasing the flexural stiffness of the slender columns via longitudinal FRP strips laterally supported by transverse FRP sheets preventing local buckling and debonding of the strips under compression.

Other solutions such as conventional transverse FRPs (wrapping system) do not contribute to the improvement of the flexural stiffness. However, they are effective for the improvement of the axial capacity of short RC columns under pure axial or low eccentric compression loadings via confining the concrete core. The lateral support provided by transverse FRPs in the hybrid system is also essential for the longitudinal FRPs preventing their premature local buckling and debonding. The confinement of concrete, provided by the FRP wrapping, also contributes to the axial capacity of the column, however, it needs to be activated as described in this study. In addition, the performance of longitudinal FRPs in compression has been under question by existing design guidelines due to the lack of experimental studies. The current study shows that longitudinal FRP can survive under compression contributing to the flexural stiffness of the slender columns to change the behavior of the columns without a premature failure under compression.

EXPERIMENTAL PROGRAM

For this study, six slender circular steel reinforced concrete (RC) columns (260x3048 mm) were designed per ACI 318-19 (2019) as presented in Fig. 1. Six 15M steel rebar with a cross-sectional area of 200 mm^2 were used as longitudinal reinforcement and twenty 10M ties were considered as ties. The spacing of ties was 203 mm in the middle of the column and reduced to 102 mm at the distance of 610 mm at the end of the columns. A normal concrete class of C30 with a nominal concrete strength of 30 MPa was designed which is close to the concrete strength of aged structures.

Test Matrix

A total of six concrete specimens were considered in this study: 1) one control specimen was considered without strengthening; 2) two wrapped specimens were considered, one with six layers of GFRP wrapping and one with two layers of CFRP wrapping; 3) three hybrid specimens were

considered with sixteen or eight longitudinal CFRP strips (50x1.2 mm) and six layers of GFRP wrapping or two layers of CFRP wrapping. To investigate the effect of different confining pressure on the behavior of the hybrid system, different wrap stiffness was provided by 6 and 2 layers of GFRP and CFRP wraps, respectively. The stiffness of FRP wrapping (i.e., $E_f t_f$) were 83 and 248 GPa.mm for six layers of GFRP and two layers CFRP wraps, respectively. The equivalent amount of GFRP wrap to produce the same stiffness as two layers of CFRP would be equal to 18 layers of GFRP. Thus, it was practical to use GFRP for both levels of confinement. It should be mentioned that 16 CFRP strips used for H-TG6-LC16 is considerably higher than what is typically expected for a real-life application, however, it was selected for the specimen to evaluate the performance of the system under an extreme scenario to see the effectiveness of the longitudinal CFRPs on flexural stiffness. This scenario can be applicable for a column with a very high slenderness ratio with a need for high flexural stiffness, however, it is not efficient to be used for columns with low slenderness. The test matrix is presented in Table 1. The specimen IDs started with the letter "W" or "H", which stands for wrapped and hybrid system, followed by the letter "T" and "L" which stand for transverse and longitudinal reinforcements, respectively. After the letter "T", the wrapping type (i.e., G for glass and C for carbon), and the number of layers was presented, and after the letter "L", the type and number of longitudinal FRP laminates is given. For example, H-TG6-LC16 is a representative of a hybrid specimen wrapped with 6 layers of GFRP wrapping and longitudinally strengthened with 16 layers of CFRP strips.

Fabrication

Fig. 2 shows the fabrication process. Steel cages were built (with the detail presented in Fig. 1) and were put inside circular cardboard tubes used as a mold, as shown in Fig. 2(a). A concrete cover of 25.4 mm was considered for the concrete section. Ready-mix concrete was poured inside

the molds with a slump of 200 mm. After the concrete was poured, the molds were not removed before 28 days to keep the moisture and have better curing. Once the molds were removed, the location of the longitudinal CFRP laminates was marked on the surface of the concrete column. The surface was cleaned using wire brushes. The adhesives were put on both the concrete surface and the surface of the CFRP laminates, then the CFRP strips were bonded to the concrete. Fig. 2(b) and 11.2(c) show the specimens with 8 and 16 longitudinal CFRP strips (50 x 1.2 mm), respectively. It should be noted that the CFRP strips were cut to have a length of 3000 mm which was shorter than the length of columns, to avoid their disturbance at the ends of the specimens where the loading is applied. For specimens with 8 CFRP strips, the spaces between every two strips were filled with adhesives to make the columns section circular and avoid sharp tips of CFRP strips. After longitudinal CFRPs were installed on the concrete, the specimens were wrapped with GFRP or CFRP wrapping, as shown in Fig. 2(d). It should be mentioned that 100 mm of overlap for wrapping was considered for all wrapped and hybrid specimens. Also, three layers of additional wrapping with a length of 300 mm was considered for the ends of all specimens to avoid premature failure at the ends of the columns. The final shape of the hybrid specimens before testing is presented in Fig. 2(e) and 11.2(f) for glass and carbon wrapping, respectively.

Material Properties

To mimic aged structures that required retrofitting, a target concrete class of C30 was selected. Ready-mix concrete was poured for columns which showed a 28-day concrete strength of 29.4 ± 0.9 MPa and a concrete strength of 33.0 ± 0.7 MPa at the time of testing. The tensile strength and modulus of elasticity of CFRP wrapping, GFRP wrapping, and premanufactured CFRP laminate were determined by coupon tests per ASTM D3039M-14 (2014). The compressive behavior of premanufactured CFRP laminate was determined by testing compression coupons prepared and

tested per ASTM D6641M-16 (2016); the detail of tests can be found in previous research by the same research group (Khorramian and Sadeghian, 2019). The compressive and tensile material characteristics for the material used in this study are presented in Table 2. It should be noted that the ply thicknesses were 1.24, 0.54, and 1.2 mm for CFRP wrap, GFRP wrap, and CFRP premanufactured laminate, respectively.

Test Set-up and Instrumentation

Fig. 3 presents the test set-up and instrumentation. The test set-up consisted of two strong concrete cubes named "End blocks" which were tightened to the strong floor. Between these two end blocks, the load was applied to the system via a 2MN Instron actuator whose force was recorded by the load cell, as shown in Fig. 3. The columns were loaded using a displacement control approach with a rate of 2 mm/min. The load transferred from the actuator to a shaft, whose direction of movement was controlled by a tunnel. At the ends of the columns, some group bags with a thickness of 5 mm were provided and put on the surface of the concrete column and at the top and bottom of the columns. While the grout was fresh, steel caps were tightened at both ends of the columns. Once the grout was set, the ends of the columns and the steep caps work together with more integrity. At the end of the steel caps, a thick plate with a thickness of 25.4 mm was considered. To provide load eccentricity, two rollers with a diameter of 50.8 mm were considered at the ends of the specimen whose distance from the center of the columns gives the desired eccentricity. The rollers were in contact with a v-notched plate, with a thickness of 12.7 mm on top of the thick plate attached to the steel cap. The rollers allowed the specimens to rotate and to provide simply supported boundary conditions. To provide a specimen with easier movement and to cancel the effect of the wight of the column in the horizontal direction, two sets of steel balls were provided for the specimen that allows lateral movement, as shown in Fig. 3. To record the

data, two string pods (SPs) and two linear potentiometers (LPs) were installed at the mid-section of the column to record the lateral displacement. Also, a total of ten strain gauges were installed to record the axial strain in compression and tension sides on steel bars, CFRP strips, and GFRP wrapping, and to record the strain of GFRP wrapping in the hoop direction.

EXPERIMENTAL RESULTS AND DISCUSSION

Failure Modes

Fig. 4 shows the failed specimens and the modes of failure. For the control specimen, the loading continued up to the concrete spalling of the concrete column in the middle of the column, as presented in Fig. 4(a) and 4(d). After concrete crushed, there was a sudden drop in the axial load as for the control specimen. The specimens wrapped with GFRP did not reach the material failure at their peak load and failed due to the global buckling of the column, as presented in Fig. 4 (b). After buckling, the loading continued and the specimen tolerated loads which led to a smooth and long descending branch of the load-displacement curve, and the test finally stopped by the operator due to considerable lateral displacement. It should be mentioned that GFRP wrapped specimens did not experience wrap rupture. Instead, the matrix failure happened which showed matrix crushing in the compression side, as presented in Fig. 4 (b), and matrix rupture in the tension side, as presented in Fig. 4 (e). The same behavior was observed for the CFRP wrapped specimen [Fig. 4(i)] with the difference that no matrix crushing in the compression side was observed [Fig. 4(l)] while the matrix rupture occurred only in the tensile side [Fig. 4(k)].

For the hybrid specimen strengthened with 16 CFRP strips and wrapped with 6 layers of GFRP [Fig. 4(c)], the CFRP strip in the furthest compression side was crushed with considerable noise. However, the loading continued, and the system was able to sustain loads even after the failure of the strips in compression. It should be noted that the failure of longitudinal strips did not

lead to the failure of FRP wrapping. However, after the peak load, the longitudinal CFRP strips in the middle of the column in the compression side were debonded and initiated some small cracks in the GFRP wrapping which were progressed up to reaching the rupture of GFRP wrap as the loading continued, which is presented in Fig. 4(f). Once GFRP ruptured the axial load dropped with a steep slope which leads to the total failure of the column, as presented in Fig. 4(f and g).

For hybrid specimens strengthened with 8 CFRP strips, at the peak load noises started which is attributed to crushing or debonding of CFRP strips in the compression side. Further justification for failure of CFRP strips in compression can be found in verification part of this study using numerical modeling. The final failure position of GFRP and CFRP wrapped hybrid system strengthened with 8 CFRP strips are shown in Fig. 4 (h and j), respectively. It should be mentioned that for the CFRP wrapped column strengthened with 8 CFRPs in compression no sign of failure was observed in the compression side in the wrapping, as shown in Fig. 4(l). Also, for that hybrid specimens strengthened with 8 CFRP strips, the crushing or debonding of the furthest compressive CFRP strips happened at the middle of the column at peak load and continued to expand to the sections further than the mid-section as the loading continued after the peak load.

It should be noted for these two specimens with 8 longitudinal CFRP strips, no rupture of wrapping was observed as loading continued after the peak load, and similar behavior to the wrapped specimens was observed after the peak load. Instead, the matrix failure in tension and compression side was observed, as shown in Fig. 4(k-n). Therefore, it can be concluded that as the reinforcement ratio of longitudinal strips decreases, the post-peak behavior of the hybrid and wrapping strengthening systems became similar and will be controlled by matrix failure, while for higher reinforcement ratios, the post-peak will be controlled by wrapping rupture initiated by the failure of longitudinal strips. In other words, by decreasing the reinforcement ratio of the CFRP

strips, the hybrid system gains more ductility and avoided the rupture of FRP wrapping. To provide mechanics based justifications and evidence, rigorous analysis and verified model is required. Therefore, the modes of failure were further investigated in the verification section using the numerical model.

Comparison of Hybrid and Wrapping Systems of Strengthening

A summary of the test results of the experimental tests is presented in Table 3, which shows the axial displacement, lateral displacement, axial load, and bending moment at the peak load, after a 15% drop from the peak load, and at the end of the testing. For all specimens, the test was stopped by the user due to safety reasons that might have been caused because of excessive deformation in the columns, although the test would have continued further. However, the tests were terminated for the control specimen after the concrete spalling occurred and for the hybrid specimen with 16 CFRP strips after the GFRP wrapping ruptured. Table 3 also presents the value for the percentage gain in axial load capacity (PGA) with respect to the control specimen for both wrapped and hybrid specimens as well as the percentage gain of bending moment capacity (PGM). The results showed a considerable gain in the axial and flexural capacity of the hybrid strengthening system in comparison to the wrapping system. For hybrid specimens wrapped with GFRP, for specimens strengthened with 8 and 16 longitudinal CFRP strips, 82.2% and 96.4% extra gain in flexural capacity, and 21.8% and 50.9% extra gain in the axial capacity was experienced in comparison to specimen which was only wrapped. For hybrid specimen wrapped with CFRP, 63% and 39.5% extra gain in flexural and axial capacities was observed in comparison to the specimen wrapped only with CFRP. A summary of the test results and gain in the system is presented in Fig. 5.

Table 4 summarized a recording of strains at peak load for the tested specimens. It should be mentioned that some of the strain recordings were out of service as the loading continued. From

strain recordings, it was observed that the axial strain in the compressive side of the columns increased for the hybrid system in comparison to the wrapped system. The latter proves the additional stiffness of the columns due to the existence of the longitudinal CFRP strips. For hybrid concrete columns, the strain values were recorded using strain gauges installed on longitudinal CFRP laminates. The axial strain value recorded on the columns can be compared to the material coupon test results. A comparison between the coupon test results and the strain recording of laminates on the hybrid concrete columns revealed that CFRP laminates can reach their material level strain (i.e., 0.71%) or even exceed it. For example, for H-TG6-LC8, the strain of CFRP laminates at 0.77% due to the high lateral support provided by confining wraps, which cause additional support and lead to higher strain capacity. As an important proof on the validation of the hybrid system and survival of CFRP laminates, the finite-difference model, whose detail is presented later in this study, confirmed that the numerical load-displacement curves truncated at a strain of 0.71% (ultimate material strain) are corresponding to the steps that exist in the descending branch of the experimental load-displacement curves (as shown in Fig. 6). During the tests, there was some noise corresponding to these steps, but the strain values were not captured experimentally, as the strain gauges were out of order after the peak load.

Also, the results showed that the confining strain in the compression side was higher for the hybrid system at the peak load in comparison to the wrapping system. For example, a compressive axial strain of 0.0077 mm/mm was observed for H-TG6-LC8 which shows that the additional flexural stiffness due to the longitudinal FRP strips altered the mode of failure of only wrapped slender columns from global buckling. The latter allowed the activation of the confinement action which led to higher axial strains of confined concrete. Thus, the confinement in compression contributed more to the hybrid system than in the wrapped system. The latter can

be justified by the fact that the hoop strain of wrapping decreases from the compression side to the tension side. Thus, for only wrapped specimens, there is no balancing source of tensile forces for the satisfaction of load equilibrium in the section while for the hybrid system, longitudinal FRP strips in tension provide higher tensile forces and allow the confining device to experience more hoop strain s in compression which leads to higher compression forces due to confinement for the concrete. Therefore, the existence of strips in tension helps the system to engage the wrapping and make it more effective for eccentrically loaded columns. The latter shows that wrapping is not effective in the tension side and for cases that require higher flexural capacities, such as eccentrically loaded columns and slender columns, tensile strengthening is required to have a more efficient strengthening system.

Fig. 6 presents the axial load-lateral displacement and axial load-bending moment of the tested specimens. It was observed that the behavior of the wrapped specimens with different confinement levels was the same and similar. Since the global buckling controlled the system, higher confinement did not show to be of considerable advantage. However, by adding 8 CFRP strips to the wrapped system, the load-displacement behavior of the specimens was different. Therefore, it can be concluded that the difference between GFRP and CFRP wrapping for the hybrid system is providing the lateral support for the CFRP laminates in compression to prevent them from buckling in early stages as well as providing higher compressive stresses in concrete due to the confinement effect to be balanced by the longitudinal tensile strips. Since CFRP wrapping provides more lateral support and confinement than GFRP wrapping, the compressive longitudinal strips can continue to sustain higher load levels, the wrapping became more effective in providing the confinement due to its higher modulus of elasticity of CFRP wrapping, and the axial capacity of the CFRP wrapped is higher than GFRP wrapped hybrid specimen. Also, it was

observed that for CFRP wrapped hybrid specimen, providing more lateral support caused additional stiffness which led to lower displacement at the peak load and an increase in the slope of the load-displacement curve. The same increase in the stiffness was observed for hybrid column wrapped with GFRP, once the number of longitudinal strips increased from 8 to 16. In this case, by keeping the confinement the same, adding longitudinal strips caused lower confining strains in the compression side at the peak load, as presented in Table 4. The latter shows that by increasing the reinforcement ratio of the longitudinal strips, the additional strips in compression became more effective than wrapping in satisfying the equilibrium of the forces in the section since the capacity and stiffness increased while the confining strain in compression decreased by adding more longitudinal strips. Therefore, longitudinal CFRPs in compression worked together with the longitudinal strips in tension to increase the stiffness and capacity of the columns as the reinforcement ratio of longitudinal strips increases for a constant wrapping, while the wrapping acts more as the lateral support for the longitudinal strips in compression to avoid their buckling or debonding failure in the early stages. Also, from Fig. 6, it was observed that the load-displacement curves after peak load is steeper for the hybrid system strengthened with 16 longitudinal strips, since the rupture of GFRP wrap caused a sudden drop in the axial load, while for hybrid specimens strengthened with 8 CFRP strips, the after peak behavior is similar to the wrapped specimens and tends to continue sustaining loads even after the progressive failure of CFRP strips. To further investigate the hybrid system, a numerical study is required.

NUMERICAL STUDIES

This section presents an analytical-numerical model (one-dimensional finite difference model) to predict the behavior of slender columns strengthened using the hybrid system described in the previous sections. After verifying the model against experimental test results, a parametric study

is presented to evaluate the effect of influential parameters on the behavior of the strengthening system. It should be noted that similar numerical studies have been developed for FRP-wrapped concrete columns (Jiang and Teng, 2012a, 2012b, and 2013). The modeling of concrete columns strengthened with only longitudinal FRPs studied by Sadeghian and Fam (2015). Also, the combined action of longitudinal FRP and FRP wrapping was modeled by Khorramian and Sadeghian (2018c). However, in the current study, the effect of eccentricity reflected in the material model for confined concrete and the progressive failure of longitudinal FRPs were considered which caused removal of failed longitudinal FRP strips. Also, a load-control approach, by controlling the curvature, was used for capturing descending branch of load-displacement curves which is faster than usual displacement-control approach.

Model Description

The analytical-numerical model is an iterative second-order analysis developed in MATLAB using the integration of cross-sectional moment-curvature over the length of a concrete column under eccentric loading. The column was divided into multiple segments and an iterative procedure was considered to calculate the lateral deformation of each node at the end of the segments at any given load until the procedure converged. The requirement for the iterative procedure is the section analysis to determine the moment-curvature diagram of the column for each load step.

Moment-Curvature diagram

Cross-sectional analysis is required to find the moment-curvature diagram under a certain load level and eccentricity. Fig. 7(a) shows the cross-section of a concrete column with internal steel reinforcement and external longitudinal CFRP strips and transverse GFRP or CFRP wrapping. As shown in Fig. 7(b), the strain profile is assumed linear to obtain the strain of each component (i.e., steel, CFRP, and concrete), and a perfect bond was assumed between the components. Based on

the stress-strain behavior of each component, the corresponding stress and, in turn, the corresponding force can be computed, as shown in Fig. 7(c).

The stress-strain relation for steel reinforcement was considered as an elastic perfectly plastic model for both compression and tension. For longitudinal FRP strips, a linear elastic stress-strain relationship was considered up to the crushing of FRP in compression or its rupture in tension. For concrete, the tensile stress was neglected in all fibers and only compression stresses were considered in the analysis. To consider the effect of wrapping in the concrete strength, a confinement model for concentric loading (Khorramian, 2020) was used. To use the confined concrete model, the curve parameter can be determined for different wrap by performing an experimental study on the wrapped column (Cao et al., 2018). The strain efficiency factor which was considered as 0.7 as found from an updated experimental database (Khorramian, 2020). To account for the effect of eccentric loading, modification factors proposed by Cao et al. (2018) was used in this study. To calculate the stresses and forces corresponding to confined concrete, the section was divided into a number of concrete fibers with a thickness of d_y (set to 0.25 mm).

If a certain strain profile is given, a certain load eccentricity, and axial load, the internal forces in the section can be calculated and be used to establish the moment-curvature diagram. To capture the moment-curvature for a certain load step, the axial load can be positioned in different eccentricities (e) from zero to an arbitrary high eccentricity. Then, the depth of neutral axis (C) and the furthest compression fiber in concrete (ε_{cm}) should be changed with a proper algorithm so that the equilibrium of moments and forces is satisfied in the section. The satisfaction of equilibrium in the section for different eccentricities leads to the determination of a unique strain profile and gives the depth of neutral axis and in turn the curvature for a certain load and different eccentricities. The bending moment (M) would be calculated as the product of the axial load (P)

and the load eccentricity (e), and the curvature (φ) can be found by dividing the strain at the furthest compression fiber in concrete (ε_{cm}) by the depth of the neutral axis (C).

It should be highlighted that three modes of failure of crushing of CFRP strips in compression, rupture of CFRP strips in tension, rupture of FRP wrapping were considered as material failure. The moment-curvature curves are discontinued once one of the mentioned failure modes occurs, and the one that happens prior to the others, control the end of the moment-curvature diagram and failure mode of the specimen. Once the moment-curvature of the section at each given load step is found, an iterative procedure can be utilized to satisfy the boundary condition and find the deflection of the column at each loading stage.

Iterative Procedure

The differential equation of the column can be established by the central expansion of the relationship between the curvature and the deflection of the column. The curvature φ can be defined numerically by using the forward and backward differences about i^{th} node. As illustrated in Fig. 8, the column can be divided into n nodes and an iterative process can be used to satisfy the boundary conditions and gives the displacement profile of the whole column at a certain load step.

The displacement at node 1 and node n are zero (i.e. $\delta_1 = 0$ and $\delta_n = 0$) because the boundary condition of the column is simply supported. The displacement of the second node (δ_2) can be assumed as zero to find the displacement at node 3 (δ_3). Afterward, all the displacement can be found, using expansion of differential equation of column, and displacement of the two previous nodes and the curvature of the previous node. The curvature at each node can be found by using the moment-curvature diagram built for that certain load step. It should be noted that the moment (M_i) at each node can be calculated via multiplying the axial load at the k^{th} load step (P_k) by the sum of initial eccentricity (e_0) and the displacement at i^{th} node (δ_i) as shown in Fig. 8. An

iterative process is required to ensure that the displacement at node n (δ_n) is less than 10^{-5} mm to satisfy the boundary condition. The iterative procedure can be repeated for different levels of load to give the loading path or load-displacement curve.

In general, the load-displacement curve of a column can include both ascending and descending branches. In the ascending branch, the load can be increased up to the point that a slight additional load demands moment that is higher than the ultimate capacity of the moment-curvature diagram for those loads. This point is the peak load which can be achieved by repeating the iterative process and using smaller load steps close to peak load. It should be mentioned that in this paper, a load control approach is introduced for capturing the descending branch which is faster than the conventional displacement control approach for the descending branch. In other words, the iterative procedure illustrated in Fig. 8 can be used for the descending branch, but the search for the curvatures and displacements will be done for values greater than the previous loading stage. For the case of stability failure before material failure, decreasing load steps can be used after the peak load. The iterative process used for the ascending branch can be used with the difference that the displacement and the curvature of each point must be increased as the load decreases. Since the displacements are high in the case of stability failure, the load is decreasing, but the moment in each point of the column is increasing. The process can be followed up to reaching the peak moment in the moment-curvature diagram. After this point, by decreasing the load, a very large displacement leads to a higher moment demand than the capacity of the moment-curvature diagram, and the iterative process will not converge. It should be noted for columns with low slenderness, the corresponding moment to the peak load reaches the peak point of the moment-curvature diagram in the ascending branch of the load-displacement curve, which is corresponding to the material failure.

Model Verification

To verify the model, two different studies were selected including one independent experimental study performed by Xing et al. (2020) on eccentrically wrapped RC columns the experimental study presented in this paper. Eight confined concrete columns with a diameter of 300 mm, length to diameter ratios of 3, 6, 9, 11, and eccentricities of 25 mm, 50 mm, 100 mm and 150 mm, strengthened with 2, 4, and 6 layers of CFRP wrapping were selected from the experimental study performed by Xing et al. (2020) to verify the model, as presented in Fig. 9. The material and section properties along with more details of experimental tests can be found in the study by Xing et al. (2020). Fig. 9 showed a very good agreement between the model and experimental test results for the wrapping strengthening system. It should be mentioned that the curve parameter n, which is a polynomial constant for the stress-strain curve was set to 1.2 for verification of the model versus Xing et al. (2020).

Fig. 10 shows the verification of the model versus the experimental test results from the current study. Since the columns were tested under the pin-pin boundary condition provided by the rollers, the center to center of the rollers was considered as the length of the columns for calculations. The summary of the test values at the peak load are presented in Table 5. Three modes of failure of crushing of CFRP strips in compression, rupture of CFRP strips in tension, rupture of FRP wrapping was considered as material failure along with the global buckling of the column. For FRP-wrapped columns, once the maximum compressive strain of confined concrete reached the axial strain of confined concrete corresponding to rupture strain of FRP wraps, the material failure was considered. For hybrid system, the material failure is considered once either the longitudinal FRP in compression reached their ultimate strain or FRP wrap fails as explained. To capture the progressive failure, once any longitudinal FRP was crushed (reached their ultimate

strain), the analysis was continued with removed strips. The material failure which occurs prior to the others controlled the point at which the curves were cut in Fig. 10. In Fig. 10, for Hybrid specimens, the solid black is the experimental curve up to crushing of first longitudinal FRP strip. The solid gray curve is the analysis with removing the first strip, and the dotted black is the analysis with removing three strips. All curves were cut once longitudinal strips reached their crushing strain. It should be noted that confined concrete can pass the crushing strain of CFRP laminates (i.e., 0.71%) and reach even higher strains because of the presence of the confinement effect of the transverse FRPs, however, crushing of longitudinal laminates may affect the level of confinement at the failure of the column, especially where the failure is governed by the longitudinal laminates.

The verification files showed that a curve parameter n of 2.5 predicts the behavior of the GFRP wrapped specimens very well, while for CFRP wrapped specimens a curve parameter of 1.4 was used. The value of 2.5 is compatible with the finding the curve parameter done by minimizing the RMSE of experimental and predicted values for and experimental database (Khorramian, 2020). It should be highlighted that the curve parameter also can be determined for each different wrap characteristic by performing an experimental study on the wrapped column (Cao et al., 2018). For the hybrid specimens, the curve parameter n was selected to be compatible with the type of wrapping for verification.

Overall, the model shows a very good agreement with the experimental test results. For hybrid specimens, in addition to analyzing the specimen (complete model), the model with progressive failure of longitudinal FRPs was considered (i.e., with failure of 1 strip or 3 strips). The presented numerical model successfully captured the peak load, which was the intention of developing the current model, however, it does not predict the complete post-peak descending branch of the load-displacement curves, which may be required for seismic retrofit. A comparison

of different stress-strain curves for confined concrete under eccentric loading revealed that the model proposed by Lin and Teng (2019) is more appropriate to capture the post-peak behavior, while it may not provide the same degree of accuracy for determining the peak load (Khorramian, 2020).

As shown in Fig. 10, numerical results for only wrapped concrete columns showed global buckling which is the same as observed mode of failure in experimental part. For H-TG6-LC16, the model controlled by the crushing of the CFRP in compression. The crushing was considered for FRP during the test by a distinct noise. Since it was in the compression side, it can be either material failure or debonding followed by material failure. The material failure can be the crushing of longitudinal CFRP laminates or crushing of the epoxy matrix in the transverse FRP. The FRP crushing failure, observed in this study, was similar to a combination of transverse shear, brooming, and longitudinal splitting as presented in ASTM D6641-16 (2016). The strain of CFRP in compression also reached near the ultimate compressive strain obtained from the material test. To further investigate, the numerical model later confirmed that furthest compressive strip reached to the ultimate compressive strain at experimental peak load and then progressive failure of longitudinal strips continued and they were eliminated once they reached their ultimate compressive strain. From the comparison between the model and experimental curves, it was seen that between one to three strips were failed at the peak load of H-TG6-LC16. However, for H-TG6-LC8, the peak load is corresponding to the failure of 1 strip, and after the failure of the first strip, the progressive failure continued by the failure of 3 strips which matches the descending branch of the load-displacement curves, as presented in Fig. 10(a). For H-TC2-LC8, the experimental peak load was higher than the complete model without crushing of strips, as shown in Fig. 10(b). The fact that for hybrid system with 8 longitudinal strips, by removing the

longitudinal FRP strips which were crushed, the numerical curves can continue further on the pattern of failure of experimental curves, proves that the steps in the descending branch of the experimental load-displacement curves were corresponding to failure of different strips of longitudinal FRP while wraps were still providing confinement. For further studies, the model was used to perform a parametric study on the effect of slenderness ratio, load eccentricity, reinforcement ratio of longitudinal strips, wrapping stiffness, concrete strength, and the column diameter.

Parametric Studies

In this section, the analytical-numerical model was used to compare the effect of the hybrid versus the wrapping strengthening systems. The column was reinforced with six 15M steel rebar with a cross-sectional area of 200 mm^2. Concrete strength of 30 MPa, an eccentricity of 40 mm, a length of 3048 mm, and a diameter of 260 mm were considered. For the longitudinal strips, two different reinforcement ratios of 0.9% and 1.8% were considered, corresponding to 8 and 16 CFRP strips (25×1.2 mm), respectively, and 6 layers of GFRP was considered for wrapping. The rest of the parameters and material properties were the same as the experimental study for the base specimens, and one parameter changed at a time while other parameters were constant. It should be mentioned that for calculation of the capacity of the hybrid system, the failure of one strip and three strips of longitudinal CFRP strips from the compression side were considered in order to give a fair comparison between the capacity of the hybrid and wrapping strengthening systems.

Effect of Concrete Strength

To study the effect of concrete strength, five different concrete strength (f_c) of 30, 40, 50, 60, and 70 MPa were considered for the parametric study. Fig. 11(a) shows the effect of concrete strength, in which the gain in the axial capacity was calculated as the difference between the axial capacity

of the strengthened specimen and the control specimen, divided by the capacity of the control specimen. It was observed that the effect of strengthening for both wrapping and hybrid systems decreases as the concrete strength increases. The results showed that as concrete strength decreases, the additional gain in the capacity of the hybrid system with respect to the wrapping system increases. Thus, the hybrid system is most effective for lower concrete strengths which make the hybrid system more proper for the strengthening of the aged structures.

Also, Fig. 11(a) shows that the additional gain in the capacity of the hybrid system with respect to the wrapped system of strengthening does not change as concrete strength increases (i.e. the curves are almost parallel). For the lower reinforcement ratio, the elimination of three strips is the same as using strips only in the tension side. Thus, the contribution of confined concrete due to wrapping increases, and the section would be in equilibrium with a major contribution of wrapping in compression, the minor contribution of longitudinal CFRP strips in compression, and complete contribution of longitudinal strips in tension. As a result, the failure of strips in compression does not affect the axial capacity as their contribution was not dominant.

Effect of Slenderness Ratio

Fig. 11(b) shows the effect of slenderness ratio (λ) on the performance of the hybrid strengthening system in comparison with the wrapping system. Nine different slenderness ratios of 20, 30, 40, 50, 60, 70, 80, 90, and 100 were examined. The results showed that up to a certain slenderness ratio, adding longitudinal strips did not enhance the capacity of the hybrid strengthening system considerably compare to the wrapping system. As slenderness increases, the secondary moment effect increases, and the mode of failure changes from crushing of CFRP strips in compression to buckling. The gain in the hybrid system with respect to wrapping system increases as slenderness ratio increases while the mode of failure is crushing of FRP in compression for the hybrid system.

As the mode of failure of the hybrid system change to global buckling by increasing the slenderness ratio, the gain in the hybrid system with respect to the wrapping system became become almost similar for both hybrid systems with different reinforcement ratios (i.e. the curves tends to become parallel).

Effect of Eccentricity

Fig. 11(c) shows the effect of load eccentricity on the performance of the hybrid system. Four different eccentricity ratios (*e/D*) of 0.1, 0.3, 0.5, and 1 were examined. Overall, the results showed that as eccentricity increases, the gain of the system due to wrapping tends to zero while the axial capacity enhanced by the longitudinal strips. The gain in axial capacity decreases from the eccentricity ratio of 0.1 to 0.3 since the mode of failure changed from global buckling to crushing of longitudinal strips in compression. For CFRP wrapped specimens, for eccentricity ratios higher than 0.3, the mode of failure is crushing of longitudinal strips due to higher curvatures in the concrete cross-section.

Effect of Reinforcement Ratio of Longitudinal CFRP strips

Fig. 11(d) shows the effect of the reinforcement ratio of the longitudinal strips. Four different reinforcement ratios of 0.45%, 0.9%, 1.35%, and 1.8% corresponding to 4, 8, 12, and 16 longitudinal strips, respectively, were examined. The results showed that as the reinforcement ratio of longitudinal strips increases, the gain in the axial capacity increases. The failure of longitudinal strips causes a drop in the axial capacity of the hybrid system. This drop is larger for higher reinforcement ratios of longitudinal strips, which means the compressive strips become more effective as the number of strips increases. However, for lower reinforcement ratios of the strips, the capacity did not drop drastically by the failure of strips. Thus, the hybrid system can be assumed to work without strips in compression since the section equilibrium will be satisfied by longitudinal strips in tension and confined concrete in compression. The latter means that as

longitudinal strips are removed while the tensile strips are in place, the portion of internal compressive stresses that was tolerated by longitudinal strips will be tolerated by the confined concrete in the compression side to keep the section in equilibrium as strips fail.

Effect of wrapping stiffness

Fig. 11(e) shows the effect of wrapping stiffness (E_l) in the axial capacity of the columns. Four different wrapping stiffness were examined corresponding to 4, 6, 8, and 10 layers of GFRP wrapping. The results showed that as the wrapping stiffness increases, the gain in the axial capacity increases. Also, it was observed that the gain in the hybrid system became almost constant as wrapping stiffness increased (i.e. the lines in Fig. 11(e) became parallel). Also, as the wrapping stiffness increases the contribution of the confinement in the section equilibrium is more than longitudinal strips in compression. As a result, for specimens strengthened with 8 longitudinal strips, failure of strips did not affect the axial capacity, while for specimens strengthened with 16 longitudinal strips, as wrapping stiffness increases, failure of strips cause higher capacity for CFRP wrapped specimens.

Effect of Column Diameter

To study the effect of column diameter, four different series of specimens were designed as presented in Table 6. The specimens have almost the same slenderness ratio, steel reinforcement ratio, wrapping stiffness, and reinforcement ratio of longitudinal CFRP strips. Four different column diameters of 260 mm, 320 mm, 410 mm, and 490 mm were considered, as shown in Fig. 11(f). Overall, the results showed that as the diameter increases the effect of the hybrid system increases since a larger lever arm for tensile and compressive internal forces is provided by increasing the column diameter. The analysis continued to capture the axial capacity by progressive failure of longitudinal CFRP strips up to the middle section (i.e., when all compressive strips are removed). The results showed that as strips failed progressively, the axial capacity did

not change considerably. The latter emphasized that the confinement in compression and longitudinal strips in tension satisfied the section equilibrium, and the contribution of FRP strips in compression is less than confinement as the strips are removed. The latter strengthens the discussion in the section for the effect of the reinforcement ratio of longitudinal strips.

FUTURE STUDIES

The number of tests on the subject is limited and more experimental evidence is required to characterize the behavior of the hybrid system for the strengthening of slender columns. Therefore, more large-scale experimental tests on the behavior of slender concrete columns strengthened with the proposed hybrid system is crucial to continue the current study. The equivalent stiffness of the hybrid system and proposing simplified design equations using moment magnification method can be considered as the next step, once more experimental evidence is available. Also, a reliability analysis will be required to assess the safety of the proposed hybrid system for design applications. The performance of the wrapping system with longitudinal strips only in the tension side can be experimentally assessed and compared to the tested specimens. Also, it is known that the confinement is more effective for circular columns, while for rectangular columns the corners decrease the confinement effect. Therefore, the hybrid system and the effect of longitudinal elements for rectangular columns can be studied experimentally and numerically for slender columns to investigate the effectiveness of the introduced hybrid strengthening system. As the current study only addresses strengthening of pin-pin concrete columns, for columns in non-sway frames, or columns with different boundary condition, and all cases in which maximum moment is at the ends of the columns, the anchorage of the longitudinal FRPs should be studied. It should be mentioned that the cost efficiency of the studied hybrid system requires further studies, as the

current study only validates the performance and efficiency of the studied system to be considered as a valid option of strengthening for slender columns.

CONCLUSION

In this study, six large-scale slender circular steel-reinforced concrete columns were prepared and tested under combined axial and flexural loading. One specimen was considered as the control specimen without strengthening, two specimens were wrapped with GFRP or CFRP wraps, and three specimens were strengthened with longitudinal CFRP strips and transverse wrapping, known as the hybrid system, in this study. Also, an analytical-numerical model was developed which accounts for the nonlinearity in material and geometry, as well as accounting for the effect of eccentricity on the confinement. The following conclusions can be drawn:

- For GFRP wrapped specimens, the hybrid specimens strengthened with 8 and 16 longitudinal CFRP strips, improved the gain of the only wrapped system by providing an additional gain of 82.2% and 96.4% for flexural capacity, and 21.8% and 50.9% for axial capacity, respectively.
- For CFRP wrapped specimens, the hybrid specimens strengthened with 8 longitudinal CFRP strips, improved the gain of the only wrapped system by 63% and 39.5% for flexural and axial capacities, respectively.
- All hybrid specimens sustain loads after the peak load and did not experience catastrophic failure after the peak load. Progressive failure of longitudinal strips in compression after the peak load caused a decrease in the capacity, but not the total failure.
- The test results showed that as the reinforcement ratio of longitudinal CFRP strips increases, the axial load capacity increases, and the post-peak behavior changes. For higher reinforcement ratios of longitudinal strips, the failure of strips initiated small cracks in

GFRP wrap which progressed and ended in the form of rupture of FRP wrap while it did not happen for lower reinforcement ratio. The post-peak behavior of the hybrid system with a lower reinforcement ratio of longitudinal strips was similar to the only wrapped system.

- The test results and the result of parametric study showed that the longitudinal strips in tension and confined concrete in compression are the major contributors to the section equilibrium for lower reinforcement ratio of longitudinal strips, while the longitudinal strips in compression and tension were the major contributors to the equilibrium for higher reinforcement ratios of longitudinal strips.
- An analytical-numerical model was developed and verified against the experimental tests which showed a good agreement with the test results. The model accounts for material and geometry nonlinearity as well as considering the effect of eccentric loading on the confinement of the concrete.
- The parametric study showed that the hybrid system is more effective as slenderness increases up to a certain level, as the eccentricity increases, concrete strength decreases, wrapping stiffness increases, and reinforcement ratio of longitudinal strips increases. Also, for wider column diameters, the hybrid system is slightly more effective.

DATA AVAILABILITY STATEMENT

Some or all data, models, or code generated or used during the study are available from the corresponding author by request (including test data).

ACKNOWLEDGMENTS

Authors would like to thank Jordan Maerz and Brian Kennedy for their assistance in the lab. Also, the author would thank Raghad Kassab and Aidan McCracken for performing material tests for

CFRP and GFRP wrapped coupons. The authors would also like to acknowledge and thank NSERC and Dalhousie University for their financial support.

REFERENCES

ACI 318-19. (2019). Building Code Requirements for Structural Concrete. *Farmington Hills, MI: American Concrete Institute*.

ACI 440.1R. (2015). Guide for the Design and Construction of Structural Concrete Reinforced Fiber-Reinforced Polymer (FRP) Bars*, Farmington Hills, MI: American Concrete Institute*.

ACI 440.2R. (2017). Guide for the Design and Construction of Externally Bonded FRP Systems for Strengthening Concrete Structures. *Farmington Hills, MI: American Concrete Institute*.

Al-Nimry, H., and Soman, A. (2018). On The Slenderness And FRP Confinement of Eccentrically-Loaded Circular RC Columns. *Engineering Structures*, 164: 92-108.

Ashour, A. F., El-Refaie, S. A., and Garrity, S. W., (2004). Flexural Strengthening of RC Continuous Beams Using CFRP Laminates. *Cement and concrete composites,* 26(7): 765-775.

ASTM D3039/D3039M-14. (2014). Standard test method for tensile properties of polymer matrix composite materials. *West Conshohocken, PA, USA: American Society for Testing and Materials.*

ASTM D6641/D6641M-16. (2016). Standard test method for compressive properties of polymer matrix composite materials using a combined loading compression (CLC) test fixture. *West Conshohocken, PA, USA: American Society for Testing and Materials.*

Bisby, L., and Ranger, M. (2010). Axial–Flexural Interaction in Circular FRP-Confined Reinforced Concrete Columns. *Construction and Building Materials*, 24(9): 1672-1681.

Bournas, D. A., and Triantafillou, T. C. (2013). Biaxial Bending of Reinforced Concrete Columns Strengthened with Externally Applied Reinforcement in Combination with Confinement. *ACI Structural Journal*, 110(2): 193.

Cao, Y., Wu, Y. F., and Jiang, C. (2018). Stress-Strain Relationship of FRP Confined Concrete Columns Under Combined Axial Load and Bending Moment. *Composites Part B: Engineering*, 134: 207-217.

Carrazedo, R., and de Hanai, J. B. (2017). Concrete Prisms and Cylinders Wrapped by FRP Loaded in Compression with Small Eccentricities. *Journal of Composites for Construction*, 21(4): 04016115.

Chikh, N., Benzaid, R., and Mesbah, H. (2012). An Experimental Investigation of Circular RC Columns with Various Slenderness Confined with CFRP Sheets. *Arabian Journal for Science and Engineering*, 37(2): 315-323.

CSA S806. (2012). Design and Construction of Building Structures with Fibre-Reinforced Polymers. Canadian Standards Association.

Cui, C., and Sheikh, S. A. (2010). Experimental Study of Normal-And High-Strength Concrete Confined with Fiber-Reinforced Polymers. *Journal of Composites for Construction*, 14(5): 553-561.

El Maaddawy, T., El Sayed, M., and Abdel-Magid, B. (2010). The Effects of Cross-Sectional Shape and Loading Condition on Performance of Reinforced Concrete Members Confined with Carbon Fiber-Reinforced Polymers. *Materials & Design (1980-2015)*, 31(5): 2330-2341.

El-Maaddawy, T. (2009). Strengthening of Eccentrically Loaded Reinforced Concrete Columns with Fiber-Reinforced Polymer Wrapping System: Experimental Investigation and Analytical Modeling. *Journal of Composites for Construction*, 13(1): 13-24.

El-Maaddawy, T., and El-Dieb, A. S. (2011). Near-Surface-Mounted Composite System for Repair and Strengthening of Reinforced Concrete Columns Subjected to Axial Load and Biaxial Bending. *Journal of composites for construction*, 15(4): 602-614.

Fitzwilliam, J., and Bisby, L. A. (2010). Slenderness Effects on Circular CFRP Confined Reinforced Concrete Columns. *Journal of Composites for Construction*, 14(3): 280-288.

Gadjosova, K., and Bilcik, J. (2013). Full-Scale Testing of CFRP-Strengthened Slender Reinforced Concrete Columns. *Journal of composites for construction*, 17: 239-248.

Hadi, M. N. (2007). Behaviour of FRP Strengthened Concrete Columns under Eccentric Compression Loading. *Composite Structures*, 77(1), 92-96.

Hadi, M. N. S., (2006). Behaviour of FRP Wrapped Normal Strength Concrete Columns under Eccentric Loading. *Composite Structures,* 72(4): 503-511.

Issa, M. A., Alrousan, R. Z., and Issa, M. A. (2009). Experimental and parametric study of circular short columns confined with CFRP composites. *Journal of Composites for Construction*, 13(2): 135-147.

Jiang, T., and Teng, J. G. (2013). Behavior and design of slender FRP-confined circular RC columns. *Journal of Composites for Construction*, 17(4): 443-453.

Jiang, T., and Teng, J. G. (2012a). Slenderness limit for short FRP-confined circular RC columns. *Journal of Composites for Construction*, 16(6): 650-661.

Jiang, T., and Teng, J. G. (2012b). Theoretical model for slender FRP-confined circular RC columns. *Construction and building materials*, 32: 66-76.

Karimi, K., Tait, M. J., and El-Dakhakhni, W. W. (2012). Influence of Slenderness on The Behavior of a FRP-Encased Steel-Concrete Composite Column. *Journal of Composites for Construction*, 16(1): 100-109.

Khorramian K. (2020). Short and Slender Concrete Columns Internally or Externally Reinforced with Longitudinal Fiber-Reinforced Polymer Composites, *Ph.D. Thesis*. *Department of Civil and Resource Engineering, Dalhousie University, Halifax, NS, Canada.*

Khorramian, K., and Sadeghian, P. (2018a). Strengthening Short Concrete Columns Using Longitudinally Bonded CFRP Laminates. *Special Publication*, 327: 24-1.

Khorramian, K., and Sadeghian, P. (2018b). Rehabilitation of Bridge Columns using Hybrid Strengthening Method of Longitudinal CFRP and Transverse GFRP. *In 10th International Conference on Short and Medium Span Bridges (SMSB), Quebec City, QC, Canada. Canadian Society for Civil Engineering.*

Khorramian, K., and Sadeghian, P. (2018c). Strengthening Slender Circular Concrete Columns with a Novel Hybrid FRP System. *In CSCE Annual Conference 2018, Fredericton, NB, Canada. Canadian Society for Civil Engineering.*

Khorramian, K., and Sadeghian, P. (2019). Performance of High-Modulus Near-Surface-Mounted FRP Laminates for Strengthening of Concrete Columns. *Composites Part B: Engineering*, 164: 90-102.

Li, J., and Hadi, M. N. S. (2003). Behaviour of Externally Confined High-Strength Concrete Columns under Eccentric Loading. *Composite Structures*: 62(2): 145-153.

Lin, G., and Teng, J. G. (2019). Stress-Strain Model for FRP-Confined Concrete in Eccentrically Loaded Circular Columns. *Journal of Composites for Construction*, 23(3), 04019017.

Lin, G., Zeng, J. J., Teng, J. G., and Li, L. J. (2020). Behavior of Large-Scale FRP-Confined Rectangular RC Columns under Eccentric Compression. *Engineering Structures*, 216: 110759.

Nanni, A., and Bradford, N., (1995). FRP Jacketed Concrete under Uniaxial Compression. *Construction and Building Materials,* 9(2): 115-124.

NoroozOlyaee, M., and Mostofinejad, D. (2019). Slenderness Effects in Circular RC Columns Strengthened with CFRP Sheets using Different External Bonding Techniques. *Journal of Composites for Construction*, 23(1): 04018068.

Pan, J. L., Xu, T., and Hu, Z. J. (2007). Experimental Investigation of Load Carrying Capacity of The Slender Reinforced Concrete Columns Wrapped with FRP. *Construction and Building Materials*, 21(11): 1991-1996.

Parvin, A., and Wang, W. (2001). Behaviour of FRP Jacketed Concrete Columns under Eccentric Loading. *Journal of Composites for Construction*, 5(3): 146-152.

Pessiki, S., Harries, K. A., Kestner, J. T., Sause, R., and Ricles, J. M. (2001). Axial Behavior of Reinforced Concrete Columns Confined with FRP Jackets. *Journal of Composites for Construction*, 5(4): 237-245.

Quiertant, M., & Clement, J. L. (2011). Behavior of RC Columns Strengthened with Different CFRP Systems under Eccentric Loading. C*onstruction and Building Materials*, 25(2): 452-460.

Sadeghian, P. and Fam, A., (2015). Strengthening Slender Reinforced Concrete Columns using High-Modulus Bonded Longitudinal Reinforcement for Buckling Control. *Journal of structural Engineering,* 141: 04014127.

Saljoughian, A., and Mostofinejad, D. (2020). RC Columns Longitudinally Strengthened Via Novel EBRIOG Technique. *Structural Concrete*, 21(2): 570-586.

Shahawy, M., Arockiasamy, M., Beitelman, T. and Sowrirajan, R., (1996). Reinforced Concrete Rectangular Beams Strengthened with CFRP Laminates. *Composites Part B: Engineering,* 27(4): 225-233.

Sharif, A., Al-Sulaimani, G. J., Basunbul, I. A., Baluch, M. H., and Ghaleb, B. N. (1994). Strengthening of Initially Loaded Reinforced Concrete Beams using FRP Plates. *ACI structural Journal*, 91(2): 160-168.

Siddiqui, N. A., Alsayed, S. H., Al-Salloum, Y. A., Iqbal, R. A., and Abbas, H. (2014). Experimental Investigation of Slender Circular RC Columns Strengthened with FRP Composites. *Construction and Building Materials*, 69: 323-334.

Siddiqui, N., Abbas, H., Almusallam, T., Binyahya, A., and Al-Salloum, Y. (2020). Compression Behavior of FRP-Strengthened RC Square Columns of Varying Slenderness Ratios under Eccentric Loading. *Journal of Building Engineering*, 101512, In-Press.

Smith, S. T., Kim, S. J., and Zhang, H. (2010). Behavior and Effectiveness of FRP Wrap in the Confinement of Large Concrete Cylinders. *Journal of Composites for Construction*, 14(5): 573-582.

Tan, K. H. (2002). Strength Enhancement of Rectangular Reinforced Concrete Columns using Fiber-Reinforced Polymer. *Journal of Composites for Construction*, 6(3): 175-183.

Tao, Z., Teng, J. G. , Han, L.H. and Lam., L., (2004). Experimental Behaviour of FRP-Confined Slender RC Columns under Eccentric Loading. *Advanced Polymer Composites for Structural Applications in Construction.* Guildford, UK: 203-212.

Torabian, A., and Mostofinejad, D. (2017). Externally Bonded Reinforcement on Grooves Technique in Circular Reinforced Columns Strengthened with Longitudinal Carbon Fiber-Reinforced Polymer under Eccentric Loading. *ACI Structural Journal*, 114(4): 861-873.

Triantafillou, T. C., and Plevris, N. (1992). Strengthening of RC Beams with Epoxy-Bonded Fibre-Composite Materials. *Materials and Structures*, 25: 201-211.

Wang, W., Martin, P. R., Sheikh, M. N., and Hadi, M. N. (2018). Eccentrically Loaded FRP Confined Concrete with Different Wrapping Schemes. *Journal of Composites for Construction*, 22(6): 04018056.

Wu, Y. F., and Cao, Y. G. (2017). Effect of Load Path on Behavior of FRP-Confined Concrete. *Journal of Composites for Construction*, 21(4), 04017014.

Wu, Y. F., and Jiang, C. (2013). Effect of Load Eccentricity on The Stress–Strain Relationship of FRP-Confined Concrete Columns. *Composite Structures*, 98: 228-241.

Xiao, Y., and Wu, H. (2000). Compressive Behavior of Concrete Confined by Carbon Fiber Composite Jackets. *Journal of materials in civil engineering*, 12(2): 139-146.

Xing, L., Lin, G., & Chen, J. F. (2020). Behavior of FRP-Confined Circular RC Columns under Eccentric Compression. *Journal of Composites for Construction*, 24(4): 04020030.

Table 1–Test Matrix.

No.	Specimen ID	*D* (mm)	*L* (mm)	*e/h*	Steel Reinforcement	Transverse Reinforcement	Longitudinal Reinforcement
1	Control	260	3048	0.15	6-15M	-	-
2	W-TG6	260	3048	0.15	6-15M	6 layer GFRP wraps	-
3	H-TG6-LC8	260	3048	0.15	6-15M	6 layer GFRP wraps	8 CFRP strips
4	H-TG6-LC16	260	3048	0.15	6-15M	6 layer GFRP wraps	16 CFRP strips
5	W-TC2	260	3048	0.15	6-15M	2 layer CFRP wraps	-
6	H-TC2-LC8	260	3048	0.15	6-15M	2 layer CFRP wraps	8 CFRP strips

Table 2–Material properties.

Test	No.	Material Type	f (MPa)	E (GPa)	ε (mm/mm)	F_b (MPa)
Tensile test	1	CFRP laminate	3267	177.8	0.0179	-
	2	Steel bar	443	209	0.0021	-
	3	GFRP wrap	391	25.7	0.0152	-
	4	CFRP wrap	1126	100	0.0113	-
	5	Bonding adhesive*	25	4.5	0.0100	22
	6	Epoxy resin*	69	1.7	0.0406	-
Compressive test	7	CFRP laminate	1089	152.9	0.0071	-
	8	Concrete	33	-	-	-
	9	Bonding adhesive*	59.3	2.7	0.0220	22
	10	Epoxy resin*	101	2.6	0.0388	-

Note: * = the values are reported by the manufacturer. f = ultimate tensile or compressive strength; E = tensile or compressive modulus of elasticity; ε = ultimate tensile or compressive strain; F_b = bond strength.

Table 3–Summary of Test Results.

No.	Specimen ID	Load stage	Axial Displacement (mm)	Lateral Displacement (mm)	Axial Load (kN)	Bending Moment (kN-m)	PGA (%)	PGM (%)
1	Control	P_u	16.5	20.5	1152	69.76	-	-
		$0.85P_u$	-	-	-	-		
		P_{ult}	-	-	-	-		
2	W-TG6	P_u	18.3	23.2	1335	84.30	15.8	20.8
		$0.85P_u$	20.1	48.7	1134	100.58		
		P_{ult}	33.7	186.6	344	77.93		
3	H-TG6-LC8	P_u	26.1	49.3	1586	141.66	37.6	103.0
		$0.85P_u$	29.6	76.7	1348	157.29		
		P_{ult}	44.7	150.2	1059	201.55		
4	H-TG6-LC16	P_u	35.6	38.9	1921	151.51	66.7	117.2
		$0.85P_u$	44.4	82.3	1632	199.70		
		P_{ult}	47.2	105.5	779	113.34		
5	W-TC2	P_u	19.0	28.1	1335	90.96	15.8	30.4
		$0.85P_u$	21.4	59.6	1135	113.04		
		P_{ult}	56.4	285.9	248	80.97		
6	H-TC2-LC8	P_u	23.7	35.6	1789	135.27	55.3	93.9
		$0.85P_u$	26.5	63.9	1521	157.99		
		P_{ult}	50.4	215.5	541	138.13		

Note: P_u = peak load; P_{ult} = load level corresponding to ultimate displacement; PGA = Percentage gain in axial load with respect to the control specimen at the peak load; PGM = percentage gain in bending moment with respect to the control specimen at the peak load.

Table 4–Hoop and axial strains at the peak load.

No.	Specimen ID	Axial strain on FRP		Axial strain on steel		Hoop strain on FRP	
		SG_{a_c}	SG_{a_t}	SG_{a_c}	SG_{a_t}	SG_{h_c}	SG_{h_m}
1	Control*	-	-	-0.0015	0.0005	-	-
2	W-TG6	-0.0024	0.0008	-0.0023	0.0008	0.0009	0.0005
3	H-TG6-LC8	-0.0077	0.0041	-	-	0.0026	-
4	H-TG6-LC16	-0.0050	0.0024	-	0.0016	0.0021	0.0016
5	W-TC2	-0.0033	0.0013	-	0.0007	0.0005	-
6	H-TC2-LC8	-0.0062	0.0033	-	-	0.0012	-

Note: * the curvature and stiffness at peak load were calculated based on strain on steel; SG_{a_c} = axial strain in compression side; SG_{a_t} = axial strain in tension side; SG_{h_c} = hoop strain in compression side; SG_{h_m} = hoop strain in in the middle section.

Table 5– Comparison of model and test results at the peak load.

No	Column ID	Number of Failed Strips	P_u (kN)			M_u (kN-m)			Δ_u (mm)			Failure Mode
			Exp.	Mod.	Mod. /Exp.	Exp.	Mod.	Mod. /Exp.	Exp.	Mod.	Mod. /Exp.	
1	Control	-	1152	1020	0.88	69.76	59.31	0.85	20.5	18.2	0.88	GB
2	W-TG6	-	1335	1308	0.98	84.30	95.09	1.13	23.2	32.7	1.41	GB
3	W-CT2	-	1335	1343	1.01	90.96	103.6	1.14	28.1	37.1	1.32	GB
4	H-TG6-LC8	0 str.	1586	1643	1.04	141.66	132.1	0.93	49.3	40.4	0.82	GB
		1 str.		1574	0.99		125.5	0.89		39.7	0.81	GB
		3 str.		1511	0.95		112.7	0.80		34.6	0.70	GB
5	H-TG6-LC16	0 str.	1921	2054	1.07	151.51	174.6	1.15	38.9	45.0	1.16	CF
		1 str.		1971	1.03		172.8	1.14		47.6	1.23	CF
		3 str.		1810	0.94		154.9	1.02		45.6	1.17	GB
6	H-TC2-LC8	0 str.	1789	1747	0.98	135.27	148.8	1.10	35.6	45.2	1.27	CF
		1 str.		1676	0.94		150.4	1.11		49.8	1.40	GB
		3 str.		1603	0.90		143.1	1.06		49.3	1.38	GB
Mean					0.97			1.03			1.13	
STD					0.053			0.122			0.246	
COV(%)					5.46			11.89			21.83	

Note: STD = standard deviation; COV = coefficient of variation; Exp. = experimental values ; Mod. = predicted values by the model; P_u = the ultimate load; M_u = bending moment corresponding to the ultimate load; Δ_u = lateral displacement corresponding to the ultimate load; GB = global buckling; CF = crushing of CFRP strips corresponding to material failure; 0 str. = no strips failed; 1 str. = one strip failed; 3str. = three strips failed.

Table 6–Considered cases for the study of column diameter effect.

No.	Case ID	D (mm)	L (mm)	λ	Steel Reinforcement	ρ_s (%)	Transverse Reinforcement	E_l (GPa)	Longitudinal Reinforcement	ρ_f (%)
1	D260-series	260	3048	46.9	6-15M	2.26	6 layers of GFRP wrap	0.62	8 - CFRP	0.9
2	D320-series	320	3751	46.9	6-20M	2.24	7 layers of GFRP wrap	0.58	12 - CFRP	0.9
3	D410-series	410	4807	46.9	6-25M	2.27	9 layers of GFRP wrap	0.59	20 - CFRP	0.9
4	D490-series	490	5744	46.9	6-30M	2.23	11 layers of GFRP wrap	0.60	28 - CFRP	0.9

Note: D = column diameter; L = column length; λ = slenderness ratio; ρ_f = reinforcement ratio of longitudinal FRP strips; ρ_s = steel reinforcement ratio; E_l = stiffness of FRP wrap.

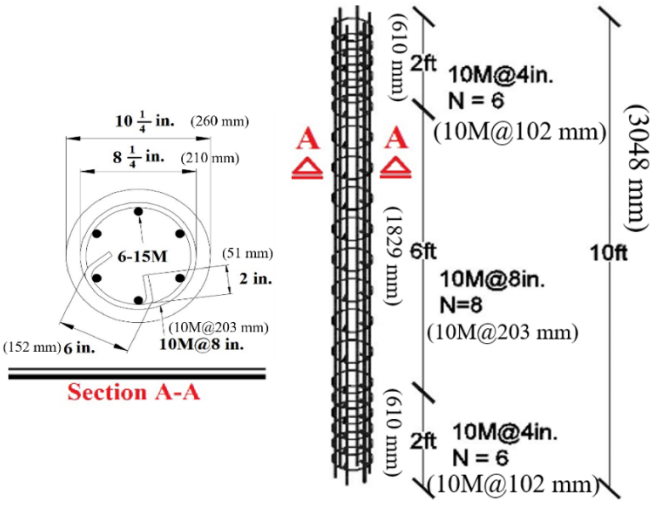

Fig. 1. Reinforcement detail.

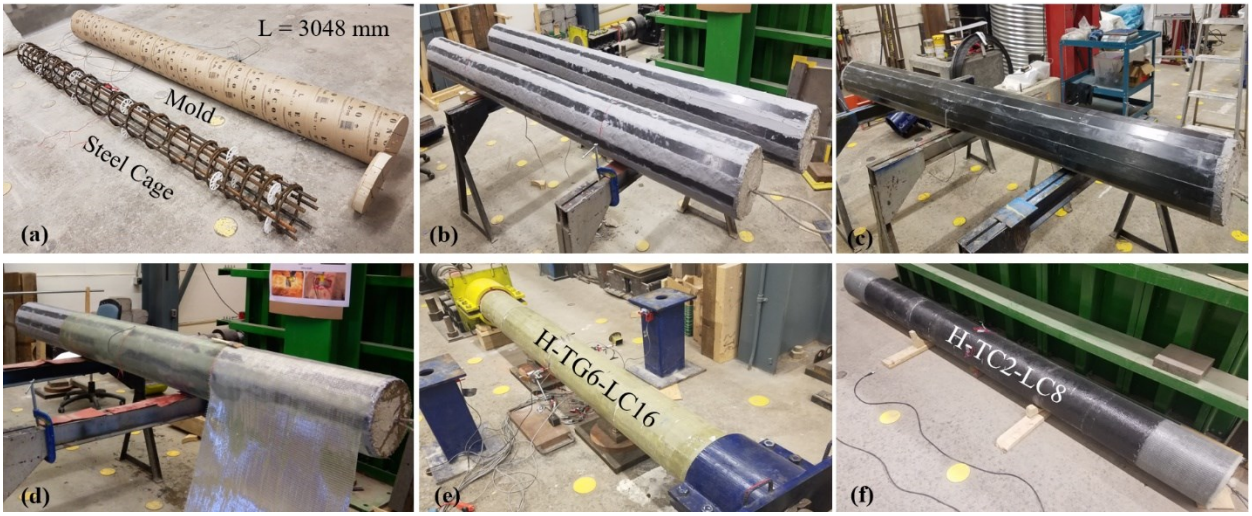

Fig. 2. Fabrication: (a) steel cage and Mold; (b) 8 CFRP strips on columns; (c) 16 CFRP strips on column; (d) Wrapping with GFRP fabric and resin; (e) Hybrid specimen with GFRP wrapping; and (f) Hybrid specimen with CFRP wrapping.

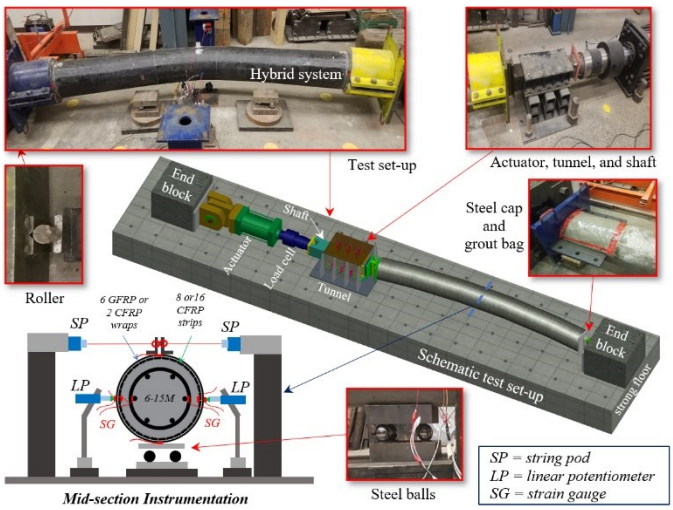

Fig. 3. Test set-up and instrumentation.

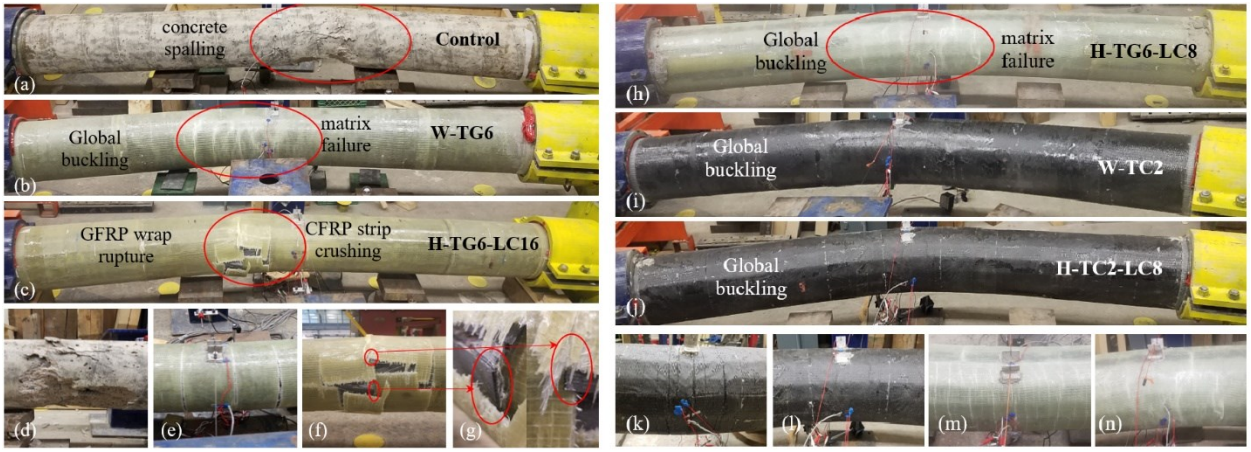

Fig. 4. Failure at ultimate state: (a) Control; (b) W-TG6; (c) H-TG6-LC16; (d) concrete spalling control specimen; (e) matrix rupture in W-TG6; (f) rupture of GFRP wrap in H-TG6-LC16; (g) crushing of CFRP strip; (h) H-TG6-LC8; (i) W-TC2; (j) H-TC2-LC8; (k) matrix rupture in tensile side of H-TC2-LC8; (l) compressive side of H-TC2-LC8; (m) tensile side of H-TG6-LC8; and (n) compressive side of H-TG6-LC8.

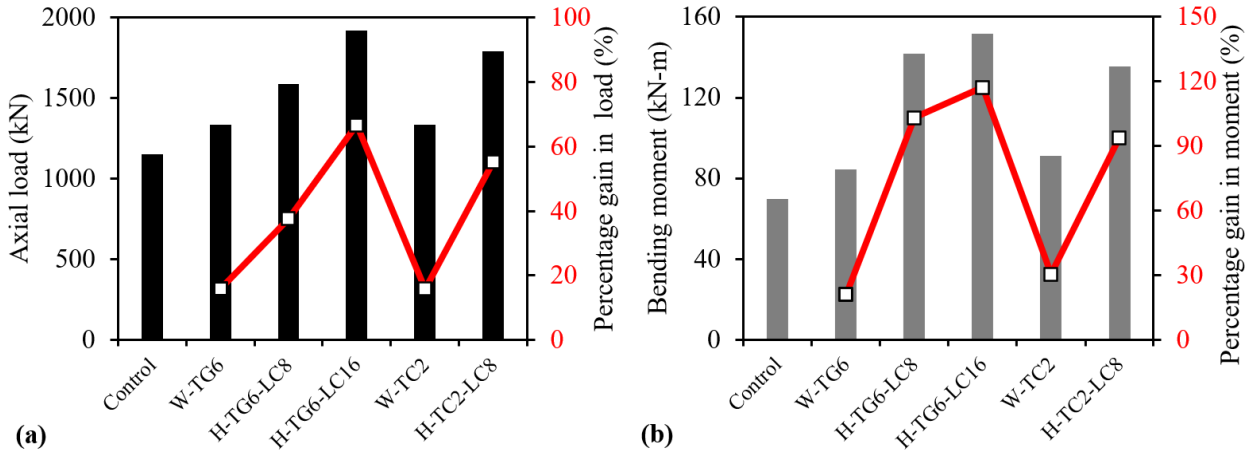

Fig. 5. Strength and gain of the tested specimens: (a) axial load capacity and gain; (b) flexural load capacity and gain.

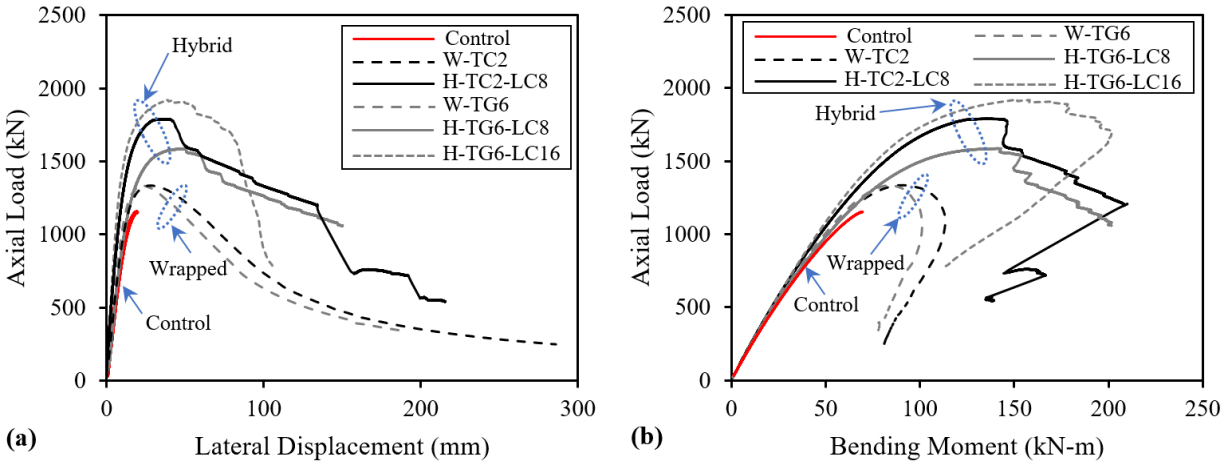

Fig. 6. Test results: (a) axial load-lateral displacement curves; and (b) axial load-bending moment curves.

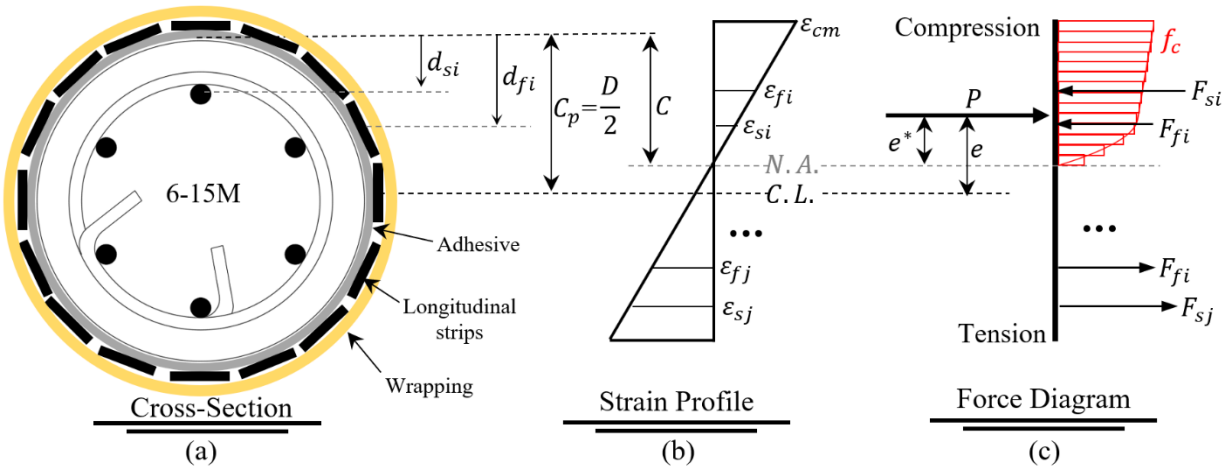

Fig. 7. Model description: (a) cross-section; (b) strain profile; and (c) Force diagram.

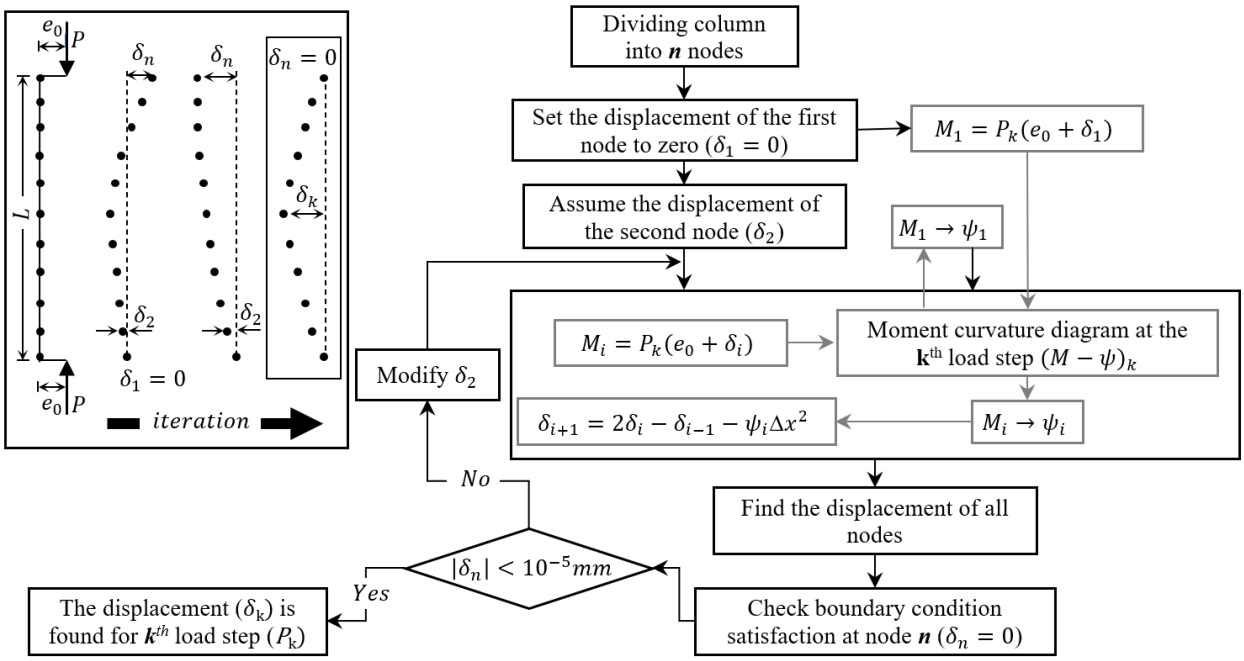

Fig. 8. Iterative Procedure for a single load step.

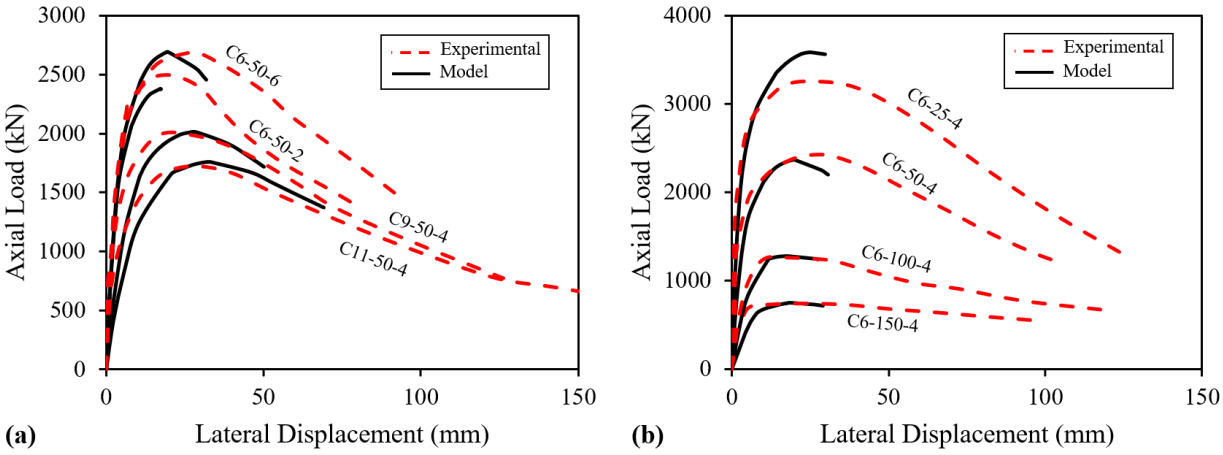

Fig. 9. Model verification for wrapped columns studied by Xing et al. (2020).

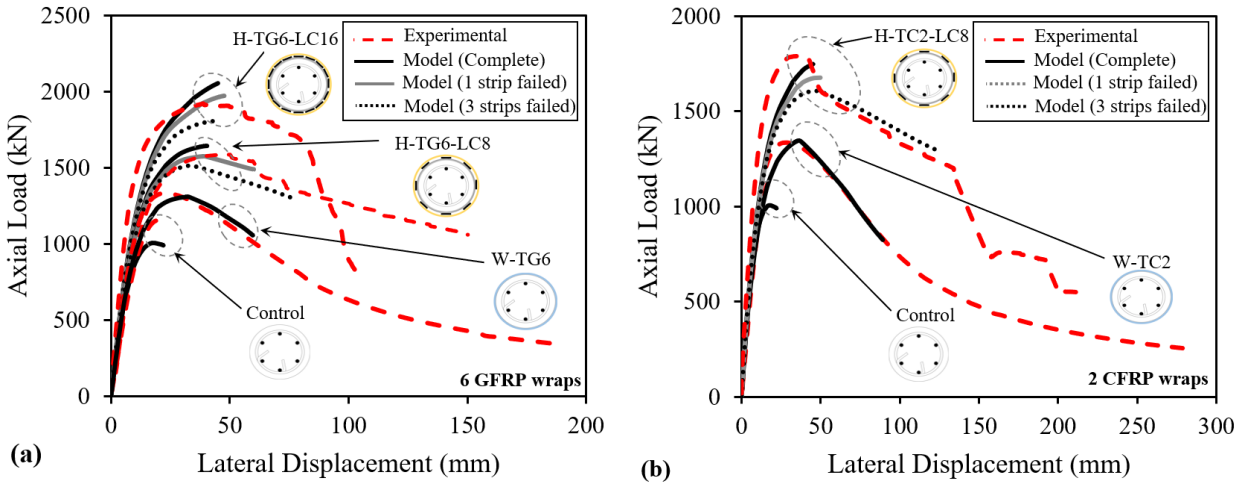

Fig. 10. Model verification against the current experimental study: (a) specimens wrapped with 6 layers of GFRP; and (b) specimens wrapped with 2 layers of CFRP.

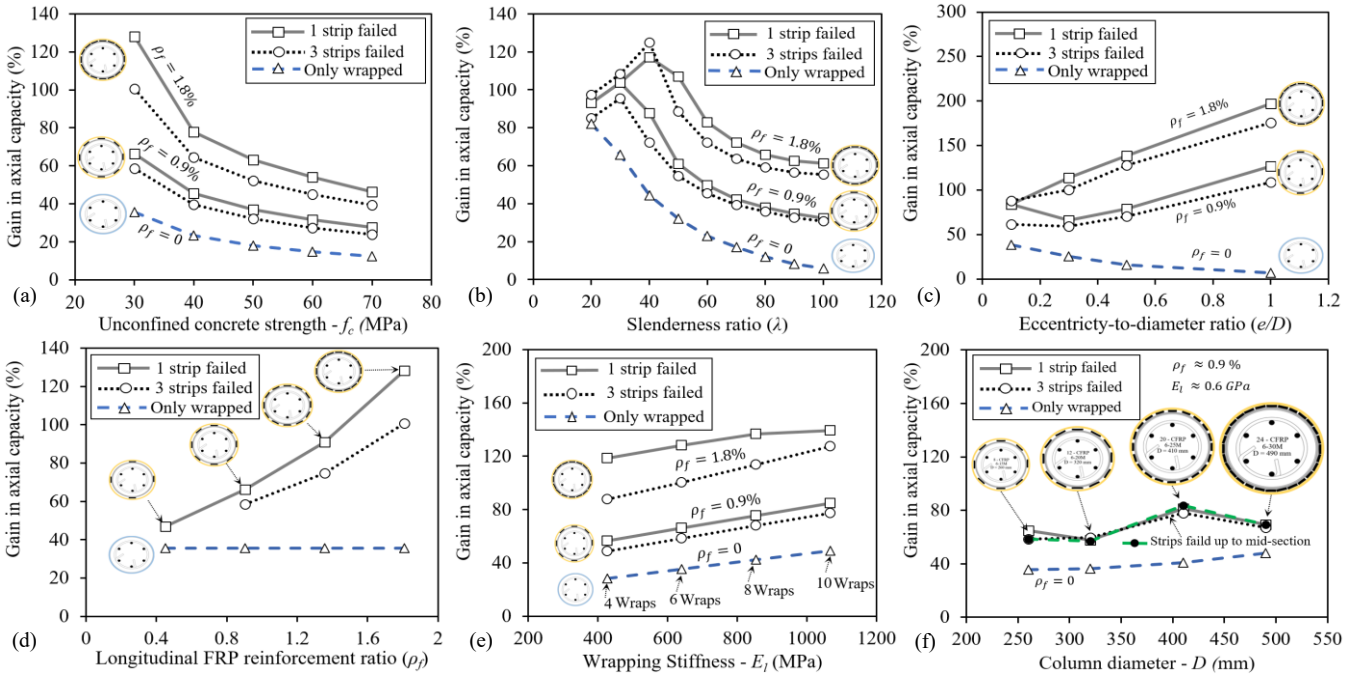

Fig. 11. Parametric study: (a) effect of concrete strength; (b) effect of slenderness ratio; (c) effect of load eccentricity; (d) effect of longitudinal FRP reinforcement ratio; (e) effect of wrapping stiffness; and (f) effect of columns diameter.